Glass Europe Vol. 3 (2025) 77-87

https://doi.org/10.52825/glass-europe.v3i.2563

Submitted: 22 Dec. 2024 | Accepted: 14 Apr. 2025 | Published: 08 May 2025

Overheating-Dependent Heterogeneous Crystal Nucleation in a Lithium Disilicate Melt

Raschid Al-Mukadam[1], Tetsuja Murata[2], Shingo Nakane[2], Hiroki Yamazaki[2], and Joachim Deubener[1,*]

[1]Institute of Non-Metallic Materials, Clausthal University of Technology, Zehnterstraße 2a, 38678 Clausthal-Zellerfeld, Germany

[2]Nippon Electric Glass, Fundamental Technology Division, 7-1 Seiran 2-Chome, Otsu, Shiga 520-8639, Japan

*Correspondence: Joachim Deubener, joachim.deubener@tu-clausthal.de

Abstract. The influence of thermal history on the kinetics of liquid-solid transformations is investigated for heterogeneous crystal nucleation near the liquidus temperature in a melt with lithium disilicate composition in contact with a PtRh10 carrier. It is shown that the achieved undercooling depends on the preceding superheating protocol. This is explained by a distribution of nano-sized cavities on the surface of the precious metal, in which crystalline clusters can persist above the liquidus temperature for a characteristic time. In series of different surface quality of the PtRh10 carrier and for air purging, these times are in the range of 5-20 s, which seems relatively long compared to metallic melts, where this phenomenon was first observed in the millisecond range. The high viscosity of the silicate melt at the liquidus temperature is discussed as the reason for the difference in the persistence time.

Keywords: Overheating, Heterogeneous Crystal Nucleation, Lithium Disilicate Glass

1. Introduction

The phenomenon that the undercooling ability of molten gallium depends on the previous overheating treatment was first described by Turnbull in 1950 [1]. He showed that at a higher temperature of the stable melt above the melting point (T_s), the occurrence of crystallisation during subsequent cooling below T_s is significantly delayed. In the following years, the phenomenon of overheating was also observed in a number of other metals and glass-forming metallic liquids, including Sn [2], [3], [4], Al [5], Bi [6], SnPb [2], $Co_{83}B_{17}$ [7] and $Zr_{52.5}Ti_5Cu_{17.9}Ni_{14.6}Al_{10}$ (Vitreloy 105) [8], [9]. The explanations are essentially based on the persistence of crystalline clusters in conical and cylindrical surface cavities in the order of nano-size of the crucible material that holds the melt [1], [3], [7], [10]. It can therefore be regarded as an artefact of hot-melt processing that can only be avoided by containerless treatment. In industrial practice, however, the contact materials for melting, handling and moulding cannot be omitted, so the overheating effect must be considered. In particular, the high temperatures in speciality glass production require precious metals based on platinum alloys, which suffer from microstructural imperfections, recrystallisation processes and mechanical stresses during manufacture and operation. Due to the non-ideality of the surface, conical and cylindrical volumes of nano size can be preferentially assumed at the bottom of scratches, at grain boundaries or at other defect structures of their surface. Besides its importance in industry, the overheating phenomenon can also play a crucial role in the determination of the liquidus temperature T_L, as most experimental procedures at high temperatures rely on an inert support material carrying liquids and crystalline samples.

Experimental proof of the overheating effect has so far only been provided for metallic systems and is still pending for oxidic (silicate) melts. However, the experiments by Burnett and Douglas [11] can be seen as a first indication of its effect on silicate melts. In their study, it was found that the undercooling limit of a melt with a composition in the barium disilicate-sodium disilicate system depends on the surface properties of the crucible material in such a way that a scratched crucible leads to crystallisation even at higher temperatures. To understand this in detail, the experimental conditions in our study were changed. For PtRh10 sheets with initial constant surface quality, different temperature-time protocols preceding the cooling step were systematically changed. From our previous work [12], [13], [14], [15] it is known that it is necessary to statistically validate the undercooling to be achieved by repeated experiments as crystal nucleation is a stochastic event.

The study is also motivated by the fact that T_L of the lithium disilicate melt with the molar composition 33.3 Li_2O, 66.7 SiO_2 from quenching experiments and thermal analyses (1306 K [16]) is at least 10 K higher than that determined by thermodynamic methods (1296 K [17], 1291 K [18]), which could possibly be due to the overheating effect. Therefore, a nearly stoichiometric lithium disilicate composition was chosen here and the time-temperature regime was adjusted so that both the experimentally determined and the thermodynamic liquidus temperature were exceeded for a certain time in each run. This means that if a decreasing delay in crystallisation occurs during subsequent cooling, this would be a clear indication that remnants of a crystal in surface cavities of the carrier material are only completely melted after longer times and higher temperatures above T_L.

2. Experiments

2.1 Glass preparation

A glass of lithium disilicate composition was melted from industrial grade lithium carbonate (Kanto Chemical Co., Ltd.) and high purity SiO_2 at 1300 °C for 2 h in air and quenched between a graphite and a cold steel plate at Nippon Electric Glass. The resulting homogeneous and transparent glass plate was immediately transferred to a muffle furnace at ~450 °C for 30 min before being carefully cooled to room temperature. The Li_2O content was determined by flame atomic absorption spectroscopy (240FS AA, Agilent Technologies, Inc.) with a relative standard deviation of about 5 %. The SiO_2 content was then calculated from the difference to 100 %. The analysed values of 33.1 Li_2O and 66.9 SiO_2 (mol %) showed only minor deviations from the target composition of $Li_2Si_2O_5$.

2.2 Heat treatment

An optical microscope (Nikon Corporation, Tokyo, Japan) with an IR imaging furnace (MS-18SP, Yonekura MFG. Co., Ltd., Osaka, Japan) was used for real-time observation of crystal growth. This high-temperature optical microscope (HTOM) is described in detail in [19]. For this purpose, a new PtRh10 sheet was cut into 26 pieces. A glass sample (~0.5 mg) was placed on each piece and attached to the sample holder of the IR imaging furnace. To create a spherical glass cap on the plate, the sample was rapidly heated to 1406 K (250 K min^{-1}), held for 5 s and then cooled at the same high rate. The sample was then ready to begin the actual experiment.

Heterogeneous crystal nucleation was studied using 3 series of different overheating experiments, each series consists of up to 11 experiments and each experiment was repeated in 30 cycles (runs) to increase statistical significance. The method was adopted from Yang et al. [3]. Each run consisted of the same temperature, heating/cooling rate and holding time above T_L, which are specified with a superscript (+) and those below T_L, which are specified with a superscript (-). To construct master curves, the total time $t_{total}^{(+)}$ above T_L was calculated as

$$t_{total}^{(+)} = \frac{\Delta T^{(+)}}{q^{(+)}{}_{heating}} + t_{hold}^{(+)} + \frac{\Delta T^{(+)}}{q^{(+)}{}_{cooling}} \quad (1)$$

where $\Delta T^{(+)}$, $q^{(+)}$ and $t_{\text{hold}}^{(+)}$ are the temperature difference, heating/cooling rate and holding time above T_{L}, respectively. While $\Delta T^{(+)}$, $q^{(+)}$ and $t_{\text{hold}}^{(+)}$ were varied between the individual experiments of a series to obtain different $t_{\text{total}}^{(+)}$, the time and temperature protocol for the undercooling was kept constant. The cooling rate below T_{L} was always 200 K min^{-1} and the heating rate below T_{L} subsequent to crystal nucleation was always 250 K min^{-1}.

An initial series of tests was carried out with a piece of PtRh10 pre-cleaned with ethanol in static air. This means that the humid air of the laboratory was enclosed in the apparatus and no purge gas was used. For all experiments in this series, the overheating temperature $\Delta T^{(+)}$ was 7 K, while $t_{\text{hold}}^{(+)}$ was increased from 1 to 38 s. For the second series, the PtRh10 plate was pre-cleaned in 46 wt% hydrofluoric acid (HF) for 1 min to remove organic residues and the passivation layer. In this series $t_{\text{hold}}^{(+)}$ was up to 1 s in static air (with one additional experiment of $t_{\text{hold}}^{(+)} = 26$ s) and $\Delta T^{(+)}$ was increased from 7 to 95 K. Finally, in the third series, PtRh10 pieces pre-cleaned with ethanol were used as in the first series, but the experiments were performed by connecting the air gun of the laboratory building's compressed air system at ~2.5 L min^{-1}. The overheating protocol included $\Delta T^{(+)}$ in the range of 6–98 K and no hold ($t_{\text{hold}}^{(+)} = 0$ s).

Figure 1 shows the section of the Li_2O-SiO_2 phase diagram with the liquidus situation near the lithium disilicate composition and the scheme of two thermal cycles of the experiments recorded in real time with the HTOM device. Table 1 compiles the experimental conditions of the three series.

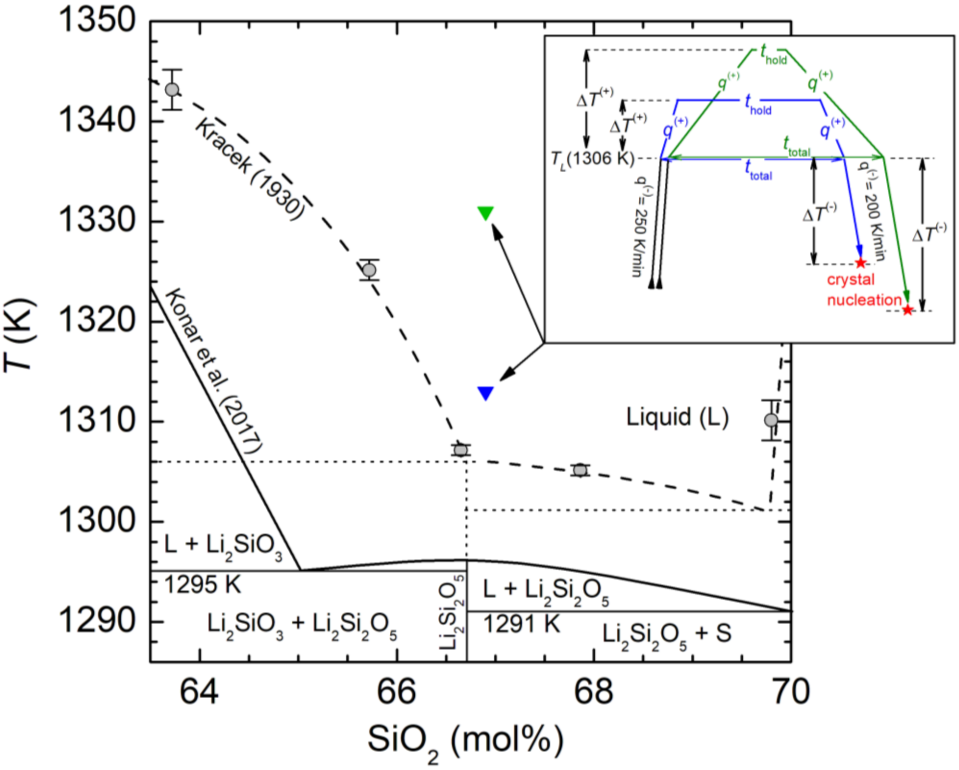

Figure 1. *Section of the Li_2O-SiO_2 phase diagram with the liquidus and solidus lines around the lithium disilicate composition ($Li_2Si_2O_5$). The solid lines are from thermodynamic calculations by Konar et al. (2017) [17], while the dashed lines and grey dots are from quenching experiments and thermal analyses by Kracek (1930) [16]. The inset exemplifies the scheme of two different thermal cycles above the liquidus with $\Delta T^{(+)} = 7$ K (blue line) and $\Delta T^{(+)} = 25$ K (green line) for the composition marked with triangles of this study.*

Table 1. *Overheating conditions of the 3 series, total time above T_L (Eq. 1), and resulting mean undercooling $\Delta T^{(-)}_{av}$ until crystal nucleation with standard deviation (σ) from 30 runs.*

$q^{(+)}$ (K min^{-1})	$\Delta T^{(+)}$ (K)	$t_{hold}^{(+)}$ (s)	$t_{total}^{(+)}$ (s)	$\Delta T^{(-)}_{av}$ (K)	σ (K)
Series I: cleaned with ethanol					
185	7	1	5.5	37.5	9.1
100	7	1	9.4	35.3	11.8
85	7	1	10.9	77.3	64.7
70	7	1	13.0	93.1	83.5
55	7	1	16.3	85.2	55.2
49	7	1	18.1	146.2	75.4
45	7	1	19.7	160.4	62.3
25	7	1	34.6	161.9	35.9
20	7	8	50.0	152.7	39.2
20	7	23	65.0	149.2	53.8
20	7	38	80.0	141.9	40.0
Series II: cleaned with HF solution					
350	7	0	2.4	28.6	10.2
350	6	1	3.1	37.0	8.6
350	9	1	4.1	117.3	70.2
500	40	0	9.6	156.6	31.7
250	47	0	22.6	176.5	45.3
250	74	0	35.5	182.3	26.1
250	95	26	45.6	186.5	19.7
110	72	0	78.5	187.0	38.8
Series III: cleaned with ethanol and air purging during experiments					
350	6	0	2.1	18.0	8.6
350	8	0	2.7	23.2	8.0
500	16.5	0	4.0	206.6	47.4
500	21	0	5.0	182.1	34.3
350	16	0	5.5	209.7	30.2
500	25	0	6.0	184.6	53.2
500	98	0	23.5	228.9	36.3

2.3 Raman spectroscopy

Reference spectra of lithium disilicate [20] and lithium metasilicate [21], [22] crystals were used to assign specific bands of the Raman spectra in the range 50–2600 cm^{-1} (RAMANtouch, Nanophoton Co., Ltd., Osaka, Japan) of the crystallised glasses. The Raman microscope was equipped with a ×20 objective and a 532 nm diode laser with a laser power of 80 mW.

3. Results

In each run, crystallites visually melted completely during heating above T_L (for the shortest heating segment of $\Delta T^{(+)} = 6$ K and $q^{(+)} = 350$ K min^{-1}, i.e. ≤ 1.03 s), so that only a homogeneous melt was observed at the overheating temperature. This melting time did not change within the 30 runs, which means that the composition of the melt remains stable throughout the experiment (negligible vaporisation of the light element lithium). The undercooling of the melt after previous overheating led to the nucleation and growth of lithium disilicate or lithium metasilicate crystallites (Figure 2) on the wetted bottom side of the melt droplet, as determined by Raman spectroscopy at the end of the experiment.

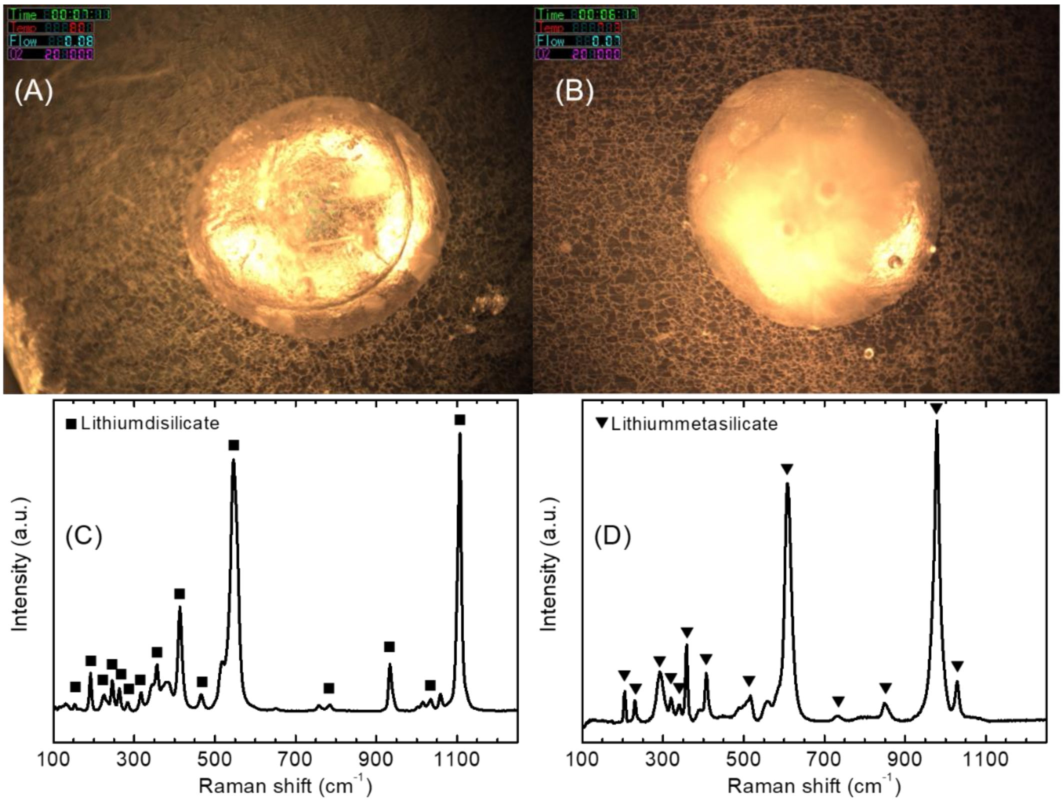

Figure 2. *Snapshots from recorded videos during the final cooling section at 200 K min^{-1} under conditions of the first series (static air / ethanol pre-cleaning of the PtRh10 sheet). Part (A) shows a transparent lithium disilicate crystallite consuming the undercooled melt, while part (B) shows opaque lithium metasilicate crystallising out. Corresponding Raman spectra of the crystallites: (C) lithium disilicate and (D) lithium metasilicate. Note the microstructure (grain boundaries) of the surface of the PtRt10 sheet.*

Figure 3 shows examples of the undercooling achieved until the onset of crystal nucleation at T_N ($\Delta T^{(-)}$ = 1306 K - T_N) in the sequence of the number of runs for 3 experiments with different preceding $t_{total}^{(+)}$ of the first series. For a relative short overheating time ($t_{total}^{(+)}$ = 5.5 s), nucleation occurred at relatively low undercooling $\Delta T^{(-)} < 50$ K in each run, while for longer overheating times of 18.1 s and 34.6 s, an increasing fraction of runs nucleated at $\Delta T^{(-)} > 50$ K. For the sake of simplicity, only the mean undercooling $\Delta T^{(-)}_{av}$ with the corresponding standard deviation σ was determined for each overheating experiment with its 30 runs and compiled in Table 1. For the determination of the heterogeneous nucleation rate see [19], [23]. A preference for lithium disilicate or lithium metasilicate crystallisation for short and long overheating times was not found. In the majority of cycles, opaque lithium metasilicate crystallites were observed first. Note that the assignment to the corresponding phases after each run was based solely on the optical appearance (cloudy-opaque versus transparent) shown in Figure 2, while confirmation by Raman spectroscopy was only obtained after the last run, as the Raman spectrometer was not coupled to the high temperature observation system. It should also be noted that the orientation of the sample with respect to the initial contact on graphite or stainless steel during splat cooling had no effect on the mean undercooling achieved.

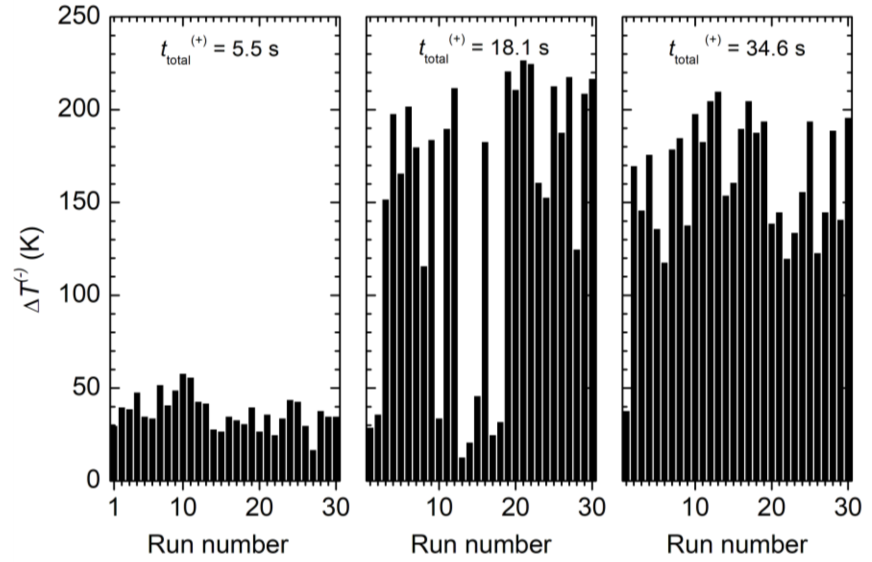

Figure 3. *Undercooling $\Delta T^{(-)}$ until nucleation and growth of lithium metasilicate and lithium disilicate crystallites in order of the run number for a preceding overheating time for 5.5 s (left), 18.1 s (centre) and 34.6 s (right) of the first series.*

Figure 4 shows the mean undercooling as a function of the total overheating time for the experiments of the first series (part A) and as a function of the overheating temperature for the second and third series (part B). It can be clearly seen that the achieved undercooling increases for short overheating times (< 20 s) and low overheating temperatures (< 15 K), but is almost constant at ~150 K for longer $t_{total}^{(+)}$ (first series) and increases only slightly at higher $\Delta T^{(+)}$ (in the range 156.6–187 K for second series and in the range 182.1–228.9 K for third series). Etching the PtRh10 sheet with HF before the experiment (black dots in Figure 4B) did not change the characteristic trend of the mean undercooling of the first series, and the use of the air flow (open triangles in Figure 4B) also led to a similar undercooling curve, however with slightly larger values.

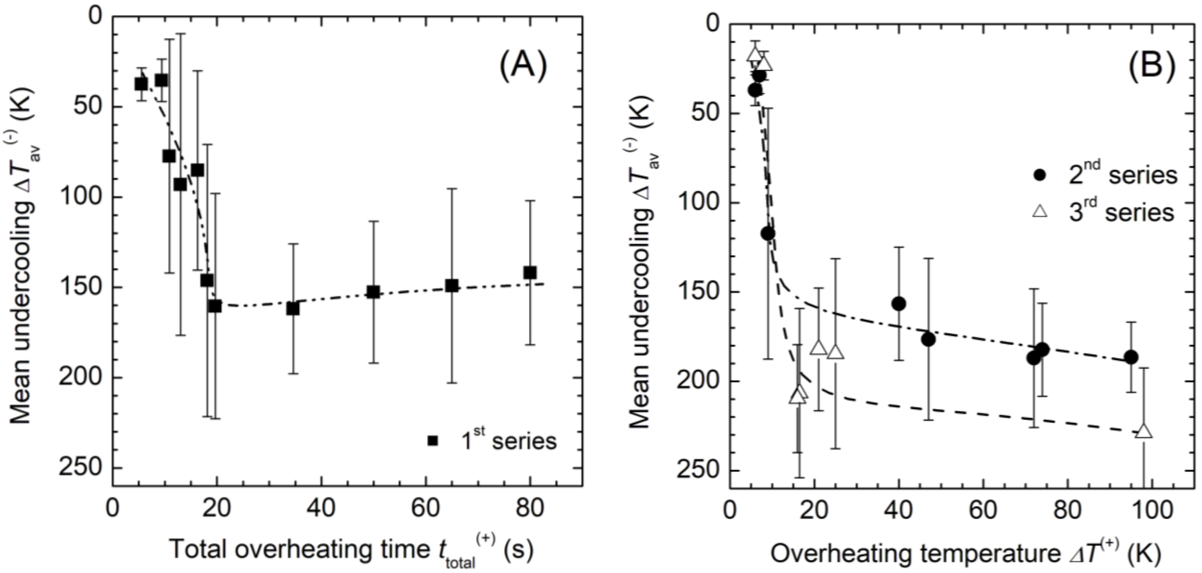

Figure 4. *Mean undercooling as a function of the preceding total overheating time (part A) and overheating temperature above T_L (part B). Dashed lines are visual guides.*

4. Discussion

Figure 5 shows the mean undercooling as a function of $t_{\mathrm{total}}^{(+)}$ for all three series together with the results for Sn from Yang et al. [3] as a reference. Obviously, a similar overheating effect can be observed for a lithium disilicate melt in contact with the PtRh10 support as for Sn. However, the overheating effect in the studied oxide system is even more pronounced than in the case of the metal tin, which nucleates heterogeneously at the interface of its own oxide skin (SnO_2) at the cavity mouth of the FDSC sensor material with a persistence time of only a few milliseconds [3]. The difference in the time scale of about 3 orders of magnitude between Sn and lithium disilicate may account due to the difference in the viscosity at T_L, i.e. 2.7×10^{-3} Pa s (Sn) [24] and 45.8 Pa s ($Li_2Si_2O_5$) [25].

As with tin, the overheating effect in lithium disilicate can be explained by the fact that during a period < 20 s (first series) and < 5 s (second and third series), optically invisible residues, i.e. crystalline clusters, are still present at some points of the surface topography, which correspond to the classical concepts of conical and cylindrical cavities [1]. At these sites, the crystalline clusters then require less time to grow to the opening of the cavity, where they build up a critical heterogeneous nucleus and grow into a visible crystallite when cooled below the liquidus temperature (see inset of Figure 5). It is further assumed that the transition from shallow to deep undercooling, as indicated by the dashed lines in Figure 5, can result from an ensemble of active cavities of different geometries.

Another aspect can be derived from the local pressure conditions. For that reason, there is hydrostatic pressure on the nanocrystal remnants in the cavities if the coefficient of thermal expansion (CTE) is greater than that of the surrounding PtRh10 sheet. A CTE of 10 ppm K^{-1} at 1000 °C is determined for the precious metal [26], while 10.4 ppm K^{-1} is specified for lithium disilicate and 15.4 ppm K^{-1} for lithium metasilicate in the range 20–400 °C for random orientation [27]. Then the effect would probably be stronger with lithium metasilicate and lead to an increase in the melting temperature according to the Clausius-Clapyeron equation. This would be consistent with the fact that lithium metasilicate crystallised more frequently in the sum of the experiments. However, there was no preference for short or long overheating times for this crystal type, which could be explained by the still low statistical significance of 30 runs per experiment. In earlier studies with higher number of runs (332), a preference for lithium disilicate at low undercooling was assumed, but the results were based on DSC, where only the crystallites of the last run can be assigned [14]. Other studies under high temperature observation also suggest this preference, but are also based on too small numbers of runs (namely 10) [28]. It should also be noted that it is not really clear which of the two phases is metastable. Recent thermodynamic calculations predict congruent melting (lithium disilicate is first on cooling) [17], but phase diagrams based on experiments show incongruent melting, i.e. lithium metasilicate is first on cooling [16].

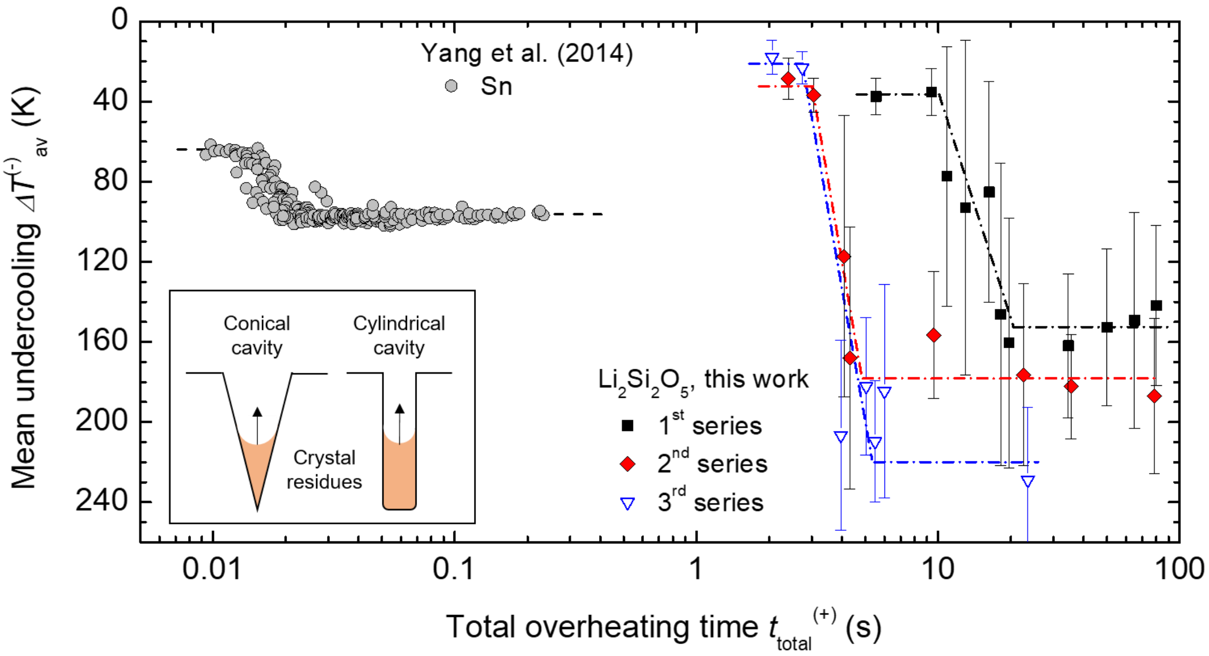

Figure 5. *Mean undercooling $\Delta T^{(-)}_{av}$ as a function of the total overheating time $t_{total}^{(+)}$ for a lithium disilicate melt in contact with the PtRh10 sheet and for liquid tin in contact with the FDSC sensor material from Yang et al. 2014 [3]. Dashed lines are visual guides. The insert schematically shows crystal residues in conical and cylindrical cavities in the sheet surface, which grow towards the mouth during undercooling (arrow).*

Figure 5 also shows that this ‘catalytic’ effect also depends on the quality of the PtRh10 surface (ethanol cleaned versus HF etched) and the atmospheric conditions (static air versus air purge) of the overheating experiments. As Figure 2 shows, the actual PtRh10 surface is not ideal but clearly has a grain boundary structure from which it can be assumed that different physical and chemical properties as well as surface topographies on a nanometre scale are present in the grain and at the grain boundary. One aspect relates to the oxidation of the precious metal alloy. It is known that the PtRh10 alloy initially forms rhodium oxides (RhO_2) on the surface at ~900 °C [29], while vaporisation of the oxide begins at over 1100 °C (0.1 Pa vapour pressure) [30]. Further, electron microscopic investigations show that the RhO_2 surface layer formed is not dense (the Pilling Bedworth ratio is 2.26) [29], [31]. It can therefore be assumed that crystal nucleation from the wetting glass melt is also influenced by the local oxidation of the PtRh10 surface which may change geometries of active cavity sites. However, further experiments are required to prove this hypothesis, as the first series was carried out at 1313 K (1040 °C) and the second and third series up to 1401 and 1404 K (1128 and 1131 °C) respectively. On the other hand, previous studies already indicated that under oxidising conditions, increasing oxygen saturation at the precious metal surface promotes low undercooling [14], [28], but the local oxygen coverage can probably only be determined by spatially resolved surface analysis (e.g. time-of-flight secondary ion mass spectrometry, TOF-SIMS), which is beyond the scope of this study.

5. Conclusions

An overheating effect was demonstrated for the first time for silicate melts and it shows that the heterogeneous crystal nucleation of lithium metasilicate in the majority of the runs, but also of lithium disilicate in the other runs, depends on the surface condition of the precious metal substrate. In particular, it is assumed that the actual metal surface has nano-sized cavities, which are active sites for the persistence of crystalline relics during overheating. Due to the high viscosity of the lithium disilicate melt at the liquidus temperature compared to molten tin, the persistence time appear to be longer (a few seconds) than with molten metal (a few milliseconds), but even more pronounced. An influence of the oxidation of the precious metal alloy cannot be ruled out, as different characteristic times of crystalline cluster persistence are found in the three test series.

Data availability statement

Data will be made available on request.

Author contributions

R. Al-Mukadam: Conceptualization, Methodology, Validation, Investigation, Writing – review & editing. T. Murata: Conceptualization, Methodology, Validation, Investigation, Writing – review & editing. S. Nakane: Writing – review & editing, Supervision, Resources. H. Yamazaki: Project administration, Funding acquisition. J. Deubener: Formal analysis, Visualization, Writing – original draft, Writing – review & editing, Supervision.

Competing interests

The authors declare that they have no competing interests.

Funding

JAPAN TRUST International Research Cooperation Project in New Energy and Industrial Technology Development Organization (NEDO) of Japan supported this work.

References

[1] D. Turnbull, “Kinetics of heterogeneous nucleation”, J. Chem. Phys., vol. 18, pp. 198–203, 1950, doi: https://doi.org/10.1063/1.1747588.

[2] H. Y. Tong and F. G. Shi, “Abrupt discontinuous relationships between supercooling and melt overheating”, Appl. Phys. Lett., vol. 70, pp. 841–843, 1997, doi: https://doi.org/10.1063/1.118220.

[3] B. Yang, J. H. Perepezko, J. W. P. Schmelzer, Y. Gao, and C. Schick, “Dependence of crystal nucleation on prior liquid overheating by differential fast scanning calorimeter”, J. Chem. Phys., vol. 140, Art. no.104513, 2014, doi: https://doi.org/10.1063/1.4868002.

[4] S. Li, L. Zhang, B. Zhao, K. Ding, and Y. Gao, “Cooling rate and roughness dependence of the undercooling for one single Sn droplet with Si thin film substrate by nanocalorimetry”, in: Characterization of minerals, metals, and materials 2022, Springer, 2022, pp. 305–314, doi: https://doi.org/10.1007/978-3-030-92373-0_29.

[5] Q. Mei and J. Li, “Dependence of liquid supercooling on liquid overheating levels of Al small particles”, Mater., vol. 9, Art. no. 7, 2015, doi: https://doi.org/10.3390/ma9010007.

[6] W. L. Webster, “Phenomena occuring in the melting of metals”, Procs. Royal Soc. London. Ser. A., vol. 140, pp. 653–660, 1933, https://doi.org/10.1098/rspa.1933.0094.

[7] J. Wang, Y. He, J. Li, R. Hu, H. Kou, and E. Beaugnon, “Overheating dependent undercooling in a hypoeutectic Co–B alloy”, Mater. Chem. Phys., vol. 149, pp. 17–20, 2015, doi: https://doi.org/10.1016/j.matchemphys.2014.11.010.

[8] X. H. Lin, W. L. Johnson, and W. K. Rhim, “Effect of oxygen impurity on crystallization of an undercooled bulk glass forming Zr–Ti–Cu–Ni–Al alloy”, Mater. Transact., vol. 38, pp. 473–477, 1997, doi: https://doi.org/10.2320/matertrans1989.38.473.

[9] S. Mukherjee, Z. Zhou, J. Schroers, W. L. Johnson, and W. K. Rhim, “Overheating threshold and its effect on time–temperature-transformation diagrams of zirconium

based bulk metallic glasses", Appl. Phys. Lett., vol. 84 pp. 5010–5012, 2004, doi: https://doi.org/10.1063/1.1763219.

[10] U. Dahlborg, M. Calvo-Dahlborg, P. S. Popel, V. E. Sidorov, "Structure and properties of some glass-forming liquid alloys", Eur. Phys. Jour. B, vol. 14, pp. 639–648, 2000, doi: https://doi.org/10.1007/s100510051073.

[11] D. G. Burnett and R. W. Douglas, "Nucleation and crystallisation in the sodia-baria-silica system", Phys. Chem. Glasses, vol. 12, pp. 117–124, 1971.

[12] S. Krüger and J. Deubener, "Stochastic nature of the liquid-to-crystal heterogeneous nucleation of supercooled lithium disilicate liquid", J. Non-Cryst. Solids, vol. 388, pp. 6–9, 2014, doi: https://doi.org/10.1016/j.jnoncrysol.2014.01.036.

[13] S. Krüger and J. Deubener, "The TTT curves of the heterogeneous and homogeneous crystallization of lithium disilicate – a stochastic approach to crystal nucleation", Front. Mater., vol. 3, Art. no. 42, 2016, doi: https://doi.org/10.3389/fmats.2016.00042.

[14] R. Al-Mukadam and J. Deubener, "Effects of cooling rate and oxygen partial pressure on heterogeneous crystal nucleation of supercooled lithium disilicate melt in PtRh20 containers", J. Non. Cryst. Solids, vol. 524, Art. no. 119642, 2019, doi: https://doi.org/10.1016/j.jnoncrysol.2019.119642.

[15] R. Al-Mukadam and J. Deubener, "Heterogeneous crystal nucleation of supercooled lithium disilicate melt in glassy carbon containers", J. Non-Cryst. Solids, vol. 571, Art. no. 121068, 2021, doi: https://doi.org/10.1016/j.jnoncrysol.2021.121068.

[16] F. C. Kracek, "The binary system lithium oxide-silica", J. Phys. Chem., vol. 34, pp. 2641–2650, 1930, doi: https://doi.org/10.1021/j150318a001.

[17] B. Konar, M. A. Van Ende, and I. H. Jung, "Critical evaluation and thermodynamic optimization of the Li-O, and Li_2O-SiO_2 systems", J. Eur. Ceram. Soc., vol. 37, pp. 2189–2207, 2017, doi: http://dx.doi.org/10.1016/j.jeurceramsoc.2016.12.041.

[18] L. Ueberricke, T. Murata, H. Ikeda, S. Nakane, and J. Deubener, "Crystal growth in oxide melts – From CALPHAD thermodynamic modeling to statistical prediction", Acta Mater., vol. 273, Art. no. 119960, 2024, doi: https://doi.org/10.1016/j.actamat.2024.119960.

[19] T. Murata, S. Nakane, H. Yamazaki, R. Al-Mukadam, and J. Deubener, "Heterogeneous crystal nucleation, viscosity and liquidus temperature in the system lithium metasilicate–lithium disilicate", J. Non-Cryst. Solids. vol. 605, Art. no. 122170, 2023, doi: https://doi.org/10.1016/j.jnoncrysol.2023.122170.

[20] S. A. Brawer and W. B. White, "Raman spectroscopic investigation of the structure of silicate glasses. I. The binary alkali silicates", J. Chem. Phys., vol. 63, pp. 2421–2432, 1975, doi: https://doi.org/10.1063/1.431671.

[21] V. Devarajan and H.F. Shurvell, "Vibrational spectra and normal coordinate analysis of crystalline lithium metasilicate", Can. J. Chem., vol. 55, pp. 2559–2563, 1977, doi: https://doi.org/10.1139/v77-353.

[22] P. Richet, B. O. Mysen, and D. Andrault, "Melting and premelting of silicates: Raman spectroscopy and X-ray diffraction of Li_2SiO_3 and Na_2SiO_3", Phys. Chem. Mineral., vol. 23, pp. 157–172, 1996, doi: https://doi.org/10.1007/BF00220727.

[23] J. Deubener and J. W. P. Schmelzer, "Statistical approach to crystal nucleation in glass-forming liquids", Entropy, vol. 23, Art. no. 246, 2021, doi: https://doi.org/10.3390/e23020246

[24] M. J. Assael, A. E. Kalyva, K. D. Antoniadis, R. M. Banish, I. Egry, J. Wu, E. Kaschnitz, and W. A. Wakeham, "Reference data for the density and viscosity of liquid copper and liquid tin", J. Phys. Chem. Ref. Data, vol. 39, Art. no. 033105, 2010, doi: https://doi.org/10.1063/1.3467496.

[25] J. Deubener and R. Brückner, "Influence of nucleation and crystallization on the rheological properties of lithium disilicate melts", J. Non-Cryst. Solids, vol. 209, pp. 96–111, 1997, doi: https://doi.org/10.1016/S0022-3093(96)00554-6.

[26] J. W. Edwards, R. Speiser, and H. L. Johnston, "High temperature structure and thermal expansion of some metals as determined by x-ray diffraction data. i. platinum, tantalum, niobium, and molybdenum", J. Appl. Phys., vol. 22, pp. 424–428, 1951, doi: https://doi.org/10.1063/1.1699977

[27] M. O. C. Villas-Boas, F. C. Serbena, V. O. Soares, I. Mathias and E. D. Zanotto, “Residual stress effect on the fracture toughness of lithium disilicate glass-ceramics”, J. Am. Ceram. Soc., 103 (2020), pp. 465-479, doi: https://doi.org/10.1111/jace.16664.
[28] M. Tashiro, S. Sukenaga, and H. Shibata, “Control of crystallization behaviour of supercooled liquid composed of lithium disilicate on platinum substrate”, Sci. Rep., vol. 7, art-no. 6078, 2017, doi: https://doi.org/10.1038/s41598-017-06306-9.
[29] A. Undisz, U. Zeigmeister, M. Rettenmayr, and M. Oechsle, “On the mechanism of internal oxidation in platinum–zirconium alloys A TEM study”, J. Alloys Comp., vol. 438 pp. 178–183, 2007, doi: https://doi.org/10.1016/j.jallcom.2006.08.036.
[30] J. V. Pearce, “Optimising platinum-rhodium thermocouple wire composition to minimise composition change due to evaporation of oxides”, Johnson Matthey Technol. Rev., vol. 60, pp. 238–242, 2016, doi: http://dx.doi.org/10.1595/205651316X692662.
[31] B. Fischer, “New platinum materials for high temperature applications”, Adv. Eng. Mater., vol. 3, pp. 811–820, 2001, doi: https://doi.org/10.1002/1527-2648(200110)3:10<811::AID-ADEM811>3.0.CO;2-%23.